DHM2020
L. Hanson et al. (Eds.)

doi:10.3233/ATDE200029

Calibration Approach for Muscle Activated Human Models in Pre-Crash Maneuvers with a Driver-in-the-Loop Simulator

Fabian KEMPTER, Florian BECHLER and Jörg FEHR[1]
University of Stuttgart, Institute of Engineering and Computational Mechanics, Pfaffenwaldring 9, 70569 Stuttgart, Germany

Abstract. Active human body models (AHBM) are essential engineering tools to provide further biomechanical knowledge. For example, to predict injury risks and kinematic behaviour in a wide range of possible scenarios such as low-g and multiaxial loading scenarios where muscle activity has shown to affect head and neck kinematics. The validation of the AHBM, in particular, the tuning and selection of an appropriate control strategy is a significant challenge. There are two main contributions of this paper. First, a Driver-in-the-Loop (DiL) simulator, used for reproducible and safe data acquisitions of human behaviour, is presented. Second, subject-specific control parameter identification to replicate the unique behaviour of each subject by using a modular calibration approach. The DiL setup is modelled in Madymo using the active human model (AHM) as a representation of the human. The Matlab/Simulink interface of Madymo is extended to implement in Matlab two new individual muscle control strategies for the head-neck region of the AHM; (i) PD controllers based on the muscle length – motivated by the equilibrium point control theory and (ii) the in-vivo stretch reflex – based on the strain measuring capabilities of the muscle spindles. Any optimization procedure available in Matlab, i.e. a particle swarm optimizer, can be used to calibrate the control parameters to achieve a good agreement between DiL measurement data and the simulation output. Finally, this modular workflow is used to identify two subject-specific sets of control parameters. These subject-specific parameters play an important role in a robust representation of human occupants.

Keywords. Active Human Body Models, Pre-Crash, Muscle Activation, Subject-Specific Calibration

1. Introduction

Traditional crash test dummy models fail to represent the dynamic behaviour of humans in integral safety concepts. Therefore, digital human models suited for the dynamic analysis of safety and comfort are becoming more critical.

For instance, realistic predicted kinematic behaviour influences the injury risk assessment in pre-crash manoeuvers. Essential in these investigations is the consideration of the active behaviour of the occupants. In [1] an overview of existing active human body models (AHBM) in the field of vehicle safety with the corresponding muscle control approach is provided. For the validation and calibration of these models, volunteer tests need to be performed and evaluated. The active control intervention and

[1] Corresponding Author, Email: joerg.fehr@itm.uni-stuttgart.de.

the chosen passive characteristics need to match real human behaviour for valid kinematic predictions. The improvements in passive properties of AHBM are not part of this work. The focus is on muscle controller parameterization, which defines the control intervention. Due to the variation in human behaviour which is pervasive in volunteer tests [2, 3] and real-world traffic, there is no characteristic controller setup which is representative of all This distribution of individual human reaction types is considered relevant to predict realistic occupants' kinematics in events of moderate acceleration values. These Pre-Crash movements of the occupants affect their injury risks and need to be accounted for in the development of future mobility solutions, where each individual is protected as best as possible.

In standard parameter identification and validation approaches, the experimental results are often averaged. Afterwards, parameter identification for the mean trajectory is performed. Nevertheless, for at least some volunteer tests the observed variance in the experimental results cannot be sufficiently modelled by a mean trajectory in addition with a variance of the identified mean parameter values, as the subject show different motion patterns. Therefore, averaging the experimental results before the identification process is debatable. In the worst-case, such an approach isn't even representative for any of the subjects.

In our approach, we try to find parameters for each individual in a first step and process the identified parameters afterwards. These individual results could be clustered to gain a set of representative controller parameterizations for different groups of human with similar characteristics, for example, level of consciousness or the individual motion strategy. Additionally, the variability of the experimental results inside the clusters can be replicated by using fuzzy valued parameters [4] instead of nominal parameter sets. In case of large data sets also information about the likelihood of parameter ranges can be considered. The behaviour of each individual itself is not the goal of our research but a first necessary step towards a more representative parameterization of AHBMs.

Current implementations of muscle controllers mainly focus on PD controllers based on joint angles in combination with spatial tuning patterns gained from experimental results, e.g. [5], – mapping angular deviations into appropriate muscle activation to decrease the control error, e.g. [1, 6]. These spatial tuning approaches need quite large input data to ensure adequate muscle activation based on angle deviations and the current posture. Alternative approaches on muscle level, like reflex control [7] or equilibrium point control [8, 9] could be beneficial in non-nominal postures because there is no need to adapt and identify spatial tuning patterns for a large variety of individual postures.

Therefore, the main contribution of this work is to present a workflow which allows the identification of individual muscle controller parameter for each individual subject. In Section 2.1, a Driver-in-the Loop setup is presented, which is used to gain the necessary experimental data for muscle parameter identification in a reproducible and safe way. In Section 2.2, the simulation setup in Madymo which emulates the experiments is presented. Afterwards, it is motivated why only a head-neck submodel is used in the identification procedure. A modular structure enabled by the Madymo coupling with Matlab/Simulink is used to parametrize and optimize the muscle level controller, which makes the workflow very flexible. The clear separation into subtasks, i.e. dynamic simulation in Madymo, muscle controller in Simulink and optimization in Matlab, increases the usability. In Section 3 Results, the experimental results of a braking scenario presented in [10] are used to calibrate the two different individual muscle neck controller. The PD control strategy and the reflex control strategy is compared. The suitability of the muscle controller definitions and the performance of the calibration approach is investigated. The paper finishes in Section 4 with a conclusion and an outlook.

2. Methods

The methods of this contribution are subdivided into three parts. i) Obtaining experimental results using a dynamical Driver-in-the-Loop simulator, ii) modelling the experimental setup in the simulation, including muscle controller and iii) optimizing the muscle controller parameters with a submodel for computational efficiency. This work combines the following software tools to a modularised workflow. The multi-body simulation performed in Madymo is separated from muscle controller modelling and parameter calibration/identification both performed in Matlab/Simulink. Furthermore, Madymo is controlled and evaluated with a Matlab-Madymo interface routine. This allows the simple adaptation of the muscle controller of each of the 136 muscle separately in Matlab/Simulink without the need of changing any input files of Madymo during the calibration/identification process.

2.1. Driver-in-the-Loop Simulator Experiments

The approach of using a DiL-simulator instead of traditional sled tests or real-car experiments possesses the following features: (i) a safe and reproducible environment, (ii) kinematic feedback in all six degrees of freedom, (iii) unconventional trajectories with superposed rotations to emulate translational accelerations, (iv) visual feedback of a virtual driving environment, e.g. by using head-mounted displays, (v) excellent accessibility for measurements and, (vi) fast application and testing of early alert systems. The whole setup is depicted in **Figure 4**. It consists of a 6-DOF motion platform, a force-feedback wheel and a bass-shaker at the back of the driving seat. The software implementation is based on a Matlab-Simulink-model, initially generated in Simcenter Prescan.

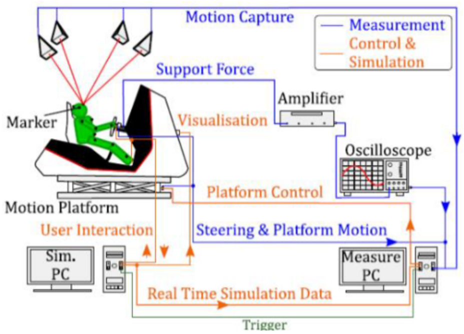

Figure 1. Driver-in-the-Loop simulator (left) with internal and external signal flow for simulation and experimental data acquisition.

Measurements. To analyze the driver's behaviour in the simulator during Pre-Crash situations, the kinematics, as well as muscle activation, can be monitored. The subjects and the simulator platform are tracked by a motion capture system Optitrack Prime with four Prime13W cameras using computer stereo vision with reflective infrared markers. Muscle activation measures are performed for the neck muscles sternocleidomastoid and trapezius using surface electromyographics [10]. Additional sensors can be applied easily using the interfaces in the Simulink model of the DiL simulation. For example, a force sensor mounted at the steering wheel allows measuring the support of the driver applied on the steering wheel [10]. This force can be considered as an indication of the amount and timing of pre-stressing in an emergency braking situation. Additionally, it affects the T1 motion and lead to head displacements. All measures are synchronized using udp or TCP/IP network communication.

Platform motion. The motion of the platform is calculated based on the state of the virtual vehicle model using motion cueing algorithms to emulate virtual vehicle accelerations [11]. Instead of performing a pure translational trajectory, in this setup, a combined translational and rotational excitation is used to emulate the vehicle accelerations. The longitudinal platform motion is extended by a superposed pitch motion **(Figure 2)**.

2.2. Modelling of the Experiments

A simulation setup of the DiL-simulator is modelled with the multibody simulation software Madymo to enable the calibration of human models with the experimental results gained in the simulator. This simulation setup is based on the default Madymo application model of a car interior with an active occupant model under gravitation of 9.81 m/s^2. The occupant is represented by the active human body model of a 50-percentile male human (1.74 m, 75.7 kg). The trajectories performed by the platform in the experiment are applied in the simulation using an ideal joint between interior parts and the inertial frame at the identical location as the platform rotational centre in the experiment, see Figure 3. First, the model needs to be initialised, with a settling run. From this settling run, a constant stimulation set $Stim_{init}$ is gained, which ensures a stable posture under gravitational load. This stimulation values $Stim_{init}$, from the settling run, will be used in all the simulations of this paper. In a subsequent simulation, the model is run with Madymo default head neck controller with the parameters (headRef = 1, reaction time = 100 ms, no co-contraction and no arm bracing). The simulation run with the full model is only performed to extract the T1 motion of the model, to enable a submodel simulation with a head-neck model, described in the following section. In the field of vehicle safety, a common approach is to investigate submodels instead of the whole human model to decrease computational cost, the number of parameters, the complexity of the simulation model and to separate effects. For studying human neck control, for instance, it can be useful to neglect the influence of changes in neck control on the upper body motion and fix the T1 motion to experimental results [1, 12, 13] or to the values gained in simulations of the whole human model with default parameterizations **(Figure 3)**. The HN-model is only applicable to identify neck controller parameters with a given T1 trajectory. Aspects influencing T1 trajectory need to be investigated separately, e.g. effects of boundary conditions or arm bracing against the steering wheel. In case of distinct arm bracing behaviour in the experimental results, the T1 trajectory of the full model needs to be reconciled before using it as an input of the HN-submodel simulations. As we aim for a separate calibration process for each subject, the reduction of computational cost of the full model (computation time 21 min 37 s) is important and can be reduced by over five times (4 min 8 s) by using a Head-Neck (HN) submodel. All the presented simulations were performed on Linux with Madymo R7.7 and Matlab/Simulink R2019b on a 12 core Intel i7-8700 processor with 3.20 GHz and 64 GB RAM.

2.2.1. Head Neck model with muscle control in Matlab/Simulink

To increase computational efficiency and to allow larger optimization runs, an extracted HN-model is derived based on the default AHBM. Muscle insertion points, which are used to be part of the upper body, are fixed to T1. The trajectory of T1 obtained in the nominal AHBM is used in the HN-model as kinematic excitation $\boldsymbol{r}_{\mathrm{T1}}^{\mathrm{HN}} := \boldsymbol{r}_{\mathrm{T1}}^{\mathrm{full}}$ (**Figure 3**). In this phase of the investigations, the influence of changes in the neck controller parameterization on the upper body motion will be neglected. In this contribution, we want to focus on muscle level controller and their suitability in reflex-based scenarios with superposed rotations. The Madymo-Simulink coupling [14] is used to allow an easier muscle controller modelling for the 136 individual muscles.

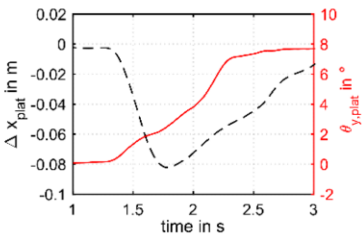

Figure 2. Platform motion longitudinal (black, dashed) and rotational (red) displacement in the braking scenario.

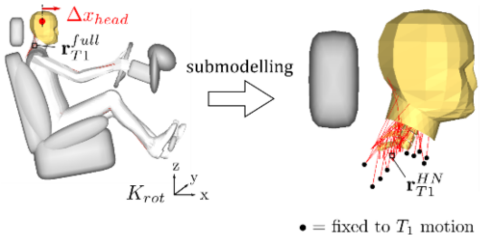

Figure 3. Madymo application model with rotational centre K_{rot} used to apply rotational and translational trajectories (left). Derived simplified HN- model with headrest and applied T1-trajectory r_{T1} (right).

While the muscle controller can be modelled more freely and intuitive in Matlab/Simulink, providing the mapping of muscle length and muscle activation signals, the dynamical simulation is performed inside the Madymo software without the need of any further adaptions during the calibration process. An overview of the Simulink structure is shown in Figure 4 exemplary for the reflex controller implementation. It consists of three main components: 1) the Madymo model with input/output definitions to Simulink, 2) the muscle controller serving the neural excitation $Stim$ at each time step based on the muscle length of the corresponding muscle element, 3) muscle activation dynamics which provides the muscle activation a based on previous activation value and neural excitation $Stim$ of the controller.

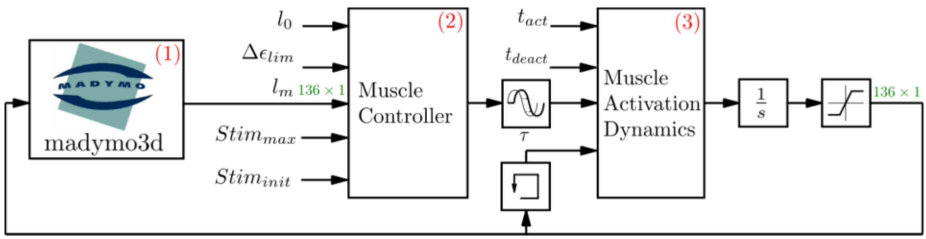

Figure 4. Structure of the Madymo-Simulink coupling: 1) Madymo transfer block with muscle activation signals a $\in \mathbb{R}^{136x1}$ as input and resultant muscle lengths at current time step l $\in \mathbb{R}^{136x1}$ as output, 2) muscle controller and 3) muscle activation dynamics.

2.2.2. Muscle Controller

In the following two muscle controller implementations are considered i) reflex controller and ii) PD controller both working only on the muscle length.

The muscle controller calculates stimulation values $Stim_i = f\left(l_i, \dot{l}_i, Stim_{\text{init},i}, p\right)$ of muscle i is a function of its length conditions, initial constant stimulation value $Stim_{\text{init},i}$ resulting from the Madymo settling run, and controller specific options p. Next, the two investigated controller definitions are described.

Reflex Controller. The reflex controller is modelled by the following relation between muscle length and muscle stimulation

$$Stim_{\text{reflex,i}} = \begin{Bmatrix} Stim_{\max} & for\ \epsilon_i > \Delta\epsilon_{\text{lim}} \\ Stim_{\text{init},i} & else \end{Bmatrix} \text{ with } \epsilon_i = \frac{l_{\text{m},i}(t-\tau) - l_{0,i}}{l_{0,i}},$$

where ϵ_i represents the strain of the muscle, τ the delay and $\Delta\epsilon_{\text{lim}}$ the strain threshold. In case of no or moderate muscle strains $\epsilon_{\text{i}} < \Delta\epsilon_{\text{lim}}$ the muscle controller is inactive and outputs the constant muscle stimulation level $Stim_{\text{init},i}$ provided as input. In the optimization procedure the parameters $Stim_{\max}$, τ and $\Delta\epsilon_{\text{lim}}$ are used as optimization parameters, as they are assumed to have the highest relevance in the used controller hypothesis to match differences in subject behaviour in reaction time τ, trigger for activating muscles $\Delta\epsilon_{\text{lim}}$ and level of counteracting $Stim_{\max}$.

PD controller. The PD muscle controller, is modelled by the following relation between the muscle activation $Stim_{\text{PD},i}$, the target value for the muscle length l_0 at the beginning of the simulation and the current (delayed) muscle length $l_{\text{m},i}$ and its derivative $\dot{l}_{\text{m},i}$

$$Stim_{\text{PD},i} = Stim_{\text{init},i} + k_p\left(\frac{l_{\text{m},i}(t-\tau) - l_{0,i}}{l_{0,i}}\right) + k_d\left(\frac{\dot{l}_{\text{m},i}(t-\tau)}{l_{0,i}}\right).$$

During the optimization process, the parameters k_{p}, k_{d} and τ are adapted.

In a first approach, the controller parameters $\Delta\epsilon_{\text{lim}}, Stim_{\max}, k_{\text{p}}$, k_{d} and τ are assumed to be equal for all muscles. An individual parametrization for muscles or muscle groups can be implemented easily but leads to increased optimization times and risk of overfitting or unphysiological parameterizations.

The activation dynamics, calculating the muscle activation a based on the neural excitation $Stim$ is modelled according to [7]. For the activation phase $t_{\text{act}} = 10\ ms$ and for the deactivation phase to $t_{\text{deact}} = 40\ ms$ is used.

2.3. Optimization

The optimization target is to decrease the deviations between simulation and experiment. In a first approach, the longitudinal head displacements Δx_{head}, expressed in coordinates of the moving platform coordinate system, are used to calculate a cost function J formulated via a mean square error

$$J = \frac{1}{m}\sum_{t_1}^{t_m}\left(\Delta x_{\text{head}}^{\text{sim}} - \Delta x_{\text{head}}^{\text{exp}}\right)^2,$$

evaluated at discrete timesteps $t_m \epsilon$ [1.2:0.01:2.2]. More proper cost functions, e.g. based on CORA evaluation [7] or multiple target signals are conceivable. Local optimization approaches with reconstructed gradients did not show good convergence behaviour. Therefore, global optimization using a particle swarm optimizer [15] in Matlab is applied to find parameter sets to minimize deviations between experimental results and simulation. The swarm size per generation is set to 20. As hybrid function the Matlab optimization routine *fmincon* is used.

3. Results

In the following, the simulation results of the head-neck model with optimized parameters are investigated. Additionally, the convergence of the optimization process is shown. Furthermore, the long-term stabilization properties of the presented muscle-controller are outlined.

3.1. Kinematic Results

The observed kinematics of one subject in a single take is compared to the HN model with the parameter sets found during optimization. In this first investigation, we considered only Δx_{head} . It is possible to consider other parameters in future investigations by adding them to the cost function calculation. The calibrated controller settings are evaluated in the time corridor t ϵ [1.2,2.2] used in the optimization process to calculate the cost function *J*. In this phase of the scenario, a good agreement can be achieved for both PD and reflex controller after optimization. Due to the lack of proportional stimulation capabilities and its on-off characteristics, the reflex controller show less smooth behaviour and higher deviations (*J*=0.0098 vs. *J*=0.0041) (**Figure 5** and Table 1. Calibrated muscle controller parameters after optimization to further investigate this issue, the mean muscle activation values of the n=136 muscles $a_{\text{mean}}(t) = \frac{1}{n}\sum_{i=1}^{n} \text{a}_i(t)$ are calculated at each timestep (**Figure 6**). The limited consistency of the reflex controller behaviour can be explained by the higher level of activation. The used reflex controller implementation with a unique stimulation level in combination with high values of τ shows excessive behaviour.

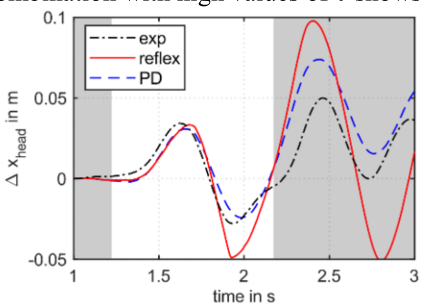

Figure 5. Head longitudinal displacement described in coordinated of the platform of simulations with optimized reflex control (red, solid) and PD control (blue dashed) in comparison to experimental target line (black dash-dotted). Only the time range of 1.2 to 2.2 s (white) is considered during optimization.

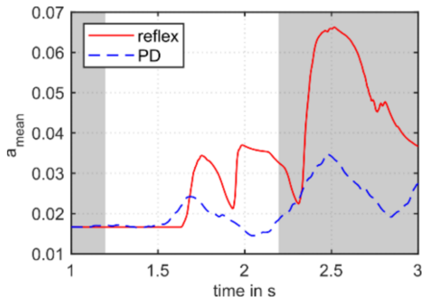

Figure 6. Mean muscle activation signals of calibrated reflex controller (red, solid) and PD controller (blue dashed). Grey shaded areas are not considered during calibration process.

Table 1. Calibrated muscle controller parameters after optimization.

Reflex controller	$\boldsymbol{Stim_{\text{max}}}$	$\boldsymbol{\Delta\epsilon_{\text{lim}}}$	**τ in s**	***J***
	0.0896	0.0154	0.1084	0.0098
PD controller	$\boldsymbol{k_p}$	$\boldsymbol{k_d}$	**τ in s**	***J***
	0.448	0.05	0.1032	0.0041

To demonstrate the robustness of the calibration approach, also the parameters of the PD controller for another subject in a single take are identified showing slightly different muscle controller parameters $\text{k}_\text{p} = 0.360$, $\text{k}_\text{d} = 0.103$ and $\tau = 0.158$, while the rating J is similar with a value of 0.0054, indicating good convergence. Due to the modularized structure of the approach, it can be applied for more complex controllers or more complex calibration tasks by extending the calculation of cost function to multiple signals and/or scenarios as well.

3.2. Convergence behaviour

In the following section, the convergence behaviour of the particle swarm optimizer is analyzed. For both reflex and PD control, the optimizer finds suitable parameter sets and converge to an optimal solution **(Figure 7)**. Starting from a broad swarm contribution in the initial population (dark blue), the parameter sets converge to optimal solutions in the later populations (red) **(Figure 8)**. In the PD controller with pure particle swarm optimization without hybrid function, the parameter k_d converges to its lower limit, while the values of k_p and τ are more spread, indicating a good exploration of the result field spanned by τ and k_p. The combined optimization approach of particle swarm optimizer with hybrid function *fmincon* used in the reflex controller shows better convergence behaviour towards the local optima, while requiring additional simulation evaluations. With the presented approach, a parameter set for one subject take can be identified with a total amount of approximately 150 simulations with computational time of 2 min 28 s each. In total, a parameter set is found approximately after six to eight hours.

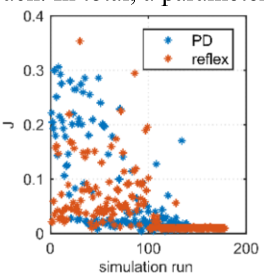

Figure 7. Convergence behaviour of the PD controller (blue) and reflex controller (red).

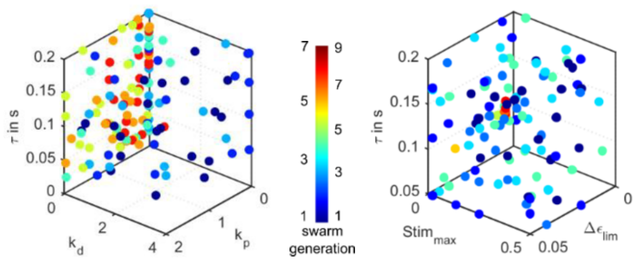

Figure 8. Contribution of data points of swarm generations during optimization. Initial population (blue) towards last swarm population (red) in optimization of PD-controller (left) and reflex-controller (right).

The expansion of the parameter space should be done cautiously. An expansion of the parameter space increases the risk of overfitting, especially if using very few evaluation sets to calculate *J*.

3.3. Long-Term Stabilization

Besides the focused phase of reflex behaviour which can be tackled quite well by the simple muscle approaches used in this study, a short outline is given to the subsequent phase. The performance and suitability for long-term stabilization of the calibrated controllers can be investigated in a time corridor that exceeds the one used in the optimization process, see the grey area in **Figure 5**. For the given data set, the calibrated PD controller shows good agreement to the experimental results. In contrast, the reflex controller seems to be less suited to enable stabilization after the initial phase.

Nevertheless, if investigating the phase after the reflex in the experimental data, there can be identified quite large deviations between the subjects. The simple controller definitions are not suited to model all the additional influences which are relevant, as for instance the control strategy or target of the individual subject. To further analyze subject-specific differences, additional experimental data with statistical evidence and evaluations of important influences is required.

4. Discussion and Outlook

The calibration and validation of active human models is a challenging topic due to the different requirements of the disciplines. Challenges are: (i) the high reproducibility and identification of representative behaviour in experimental tests and (ii) the modelling and calibration of the biomechanical models in the simulation. This contribution aims to show an approach to combine these separate subtasks in a modular way to empower users from different disciplines to improve subtasks.

In the future, large sets of calibration data with the natural variance in human behaviour will become available due to driver monitoring systems for instance. To account for this variance in the simulation models as well, semi-automatic calibration of individual subjects parameters becomes more prominent. Together with possibilistic methods, such as fuzzy valued parameters [4], the variance in experimental result can be reproduced based on individually identified parameter sets.

We presented a subject-specific identification of muscle-level controller parameters based on head kinematics gained in volunteer tests performed on a dynamic DiL-simulator. The DiL-simulator approach allows replicable investigations of driver behaviour in Pre-Crash scenarios, with and without the interaction of driver assistance systems. The transferability of the driver behaviour gained in the simulator compared to drivers in an emergent situation on the road is not finally evaluated. However, the presence of different reaction types of drivers in the simulator as well as in real cars undergoing an emergent situation is considered likely. We think that methods to address these variations can be developed and tested with data gained in the simulator, even if no direct transferability is ensured. The calibration process of the muscle-level controller using particle swarm optimizer shows good convergence behaviour, usability and good agreement in the reflex phase. However, pure muscle level control without any high-level controller seems to be less suitable for long-term stabilization tasks exceeding the human reflex phase.

Further improvements could be achieved by increasing the level of detail of the controller modelling, like different gain factors for each muscle group or a more complex cost function. For example, a CORA analysis could be performed to calculate the cost function J. Furthermore, a frequency dependency of the muscle controller could be useful to enable the emulation of human behaviour which depends on the level of external excitation or accelerations [16]. Due to the modelling as muscle-level controller, the controllers can be easily deployed in complex FE simulations. For example using the extended Hill-type muscle model presented in [17, 9].

Acknowledgement

The work presented in this paper was carried out at the Institute of Engineering and Computational Mechanics and the Cluster of Excellence Simulation Technology of the University of Stuttgart. Funded by state Baden-Wuerttemberg and the German Research Foundation (DFG) through the financial support of the project within the Juniorprofessor program and the Cluster of Excellence Simulation Technology (EXC 310/1) and Data-

Integrated Simulation Technology (EXC 2075) of the University of Stuttgart. Funded by Deutsche Forschungsgemeinschaft (DFG, German Research Foundation) under Germany's Excellence Strategy – EXC 2075 – 390740016). Additionally, the authors want to thank Francesco Labanti for his support in MADYMO modelling during his master thesis.

References

[1] Östh J, Mendoza-Vazquez M, Sato F, Svensson MY, Linder A, Brolin K. A Female Head-Neck Model for Rear Impact Simulations. Journal of Biomechanics, 2017, 51, 49–56.

[2] Bastien C, Blundell MV, Neal-Sturgess C. A Study into the Kinematic Response for Unbelted Human Occupants during Emergency Braking. International Journal of Crashworthiness, 2017, 22(6), 689–703. Available from: https://doi.org/10.1080/13588265.2017.1301080.

[3] Ghaffari G, Brolin K, Brase D, Pipkorn B, Svanberg B, Jakobsson L, et al. Passenger Kinematics in Lane Change and Lane Change with Braking Manoeuvres Using Two Belt Configurations: Standard and Reversible Pre-Pretensioner. In: Proceedings of the IRCOBI Conference. IRC-18-80. Athens, Greece, 2018, 493–511.

[4] Hanss M. The Transformation Method for the Simulation and Analysis of Systems with Uncertain Parameters. Fuzzy Sets and Systems, 2002, 130, 277–289.

[5] Ólafsdóttir JM, Brolin K, Blouin JS, Siegmund GP. Dynamic Spatial Tuning of Cervical Muscle Reflexes to Multidirectional Seated Perturbations. SPINE, 2015, 40(4), E211–E219. Available from: https://-doi.org/10.1097/brs.0000000000000721.

[6] Larsson E, Fice J, Pipkorn B, Jakobsson L, Brynskog E, Brolin K, et al. Active Human Body Model Predictions Compared to Volunteer Response in Experiments with Braking, Lane Change, and Combined Manoeuvres. In: Proceedings of the IRCOBI Conference. Florence, Italy, 2019, 349–369.

[7] Feller L, Kleinbach C, Fehr J, Schmitt S. Incorporating Muscle Activation Dynamics into the Global Human Body Model. In: Proceedings of the IRCOBI Conference. Malaga, Spain, 2016, 512–523.

[8] Kistemaker DA, Wong JD, Gribble PL. The cost of Moving Optimally: Kinematic Path Selection. Journal of Neurophysiology, 2014, 112(8), 1815–1824.

[9] Martynenko O, Kempter F, Kleinbach C, Schmitt S, Fehr J. Integrated Physiologically Motivated Controller for the Open-Source Extended Hill-type Muscle Model in LS-DYNA. In: Proceedings of the IRCOBI Conference. Athens, Greece, 2018, 239–241.

[10] Kempter F, Fehr J, Stutzig N, Siebert T. On the Validation of Human Body Models with a Driver-in-the-Loop Simulator. In: The 5th Joint Int. Conference on Multibody System Dynamics (IMSD 2018). Lisboa, Portugal, 2018, 15–31.

[11] Kempter F, Fehr J. Layout of a Driver-in-the-Loop Simulator for Validation of Human Body Models. In: Proceedings in Applied Mathematics and Mechanics, 2018.

[12] Happee R, de Bruijn E, Forbes PA, van der Helm FCT. Dynamic Head-Neck Stabilization and Modulation with Perturbation Bandwidth Investigated Using a Multisegment Neuromuscular Model. Journal of Biomechanics, 2017, 58, 203–211. Available from: http://www.sciencedirect.com/science/-article/pii/S0021929017302579.

[13] Putra IPA, Iraeus J, Thomson R, Svensson MY, Linder A, Sato F. Comparison of control strategies for the cervical muscles of an average female head-neck finite element model. Traffic Injury Prevention, 2019, 1–7. PMID: 31617760. Available from: https://doi.org/10.1080/15389588.2019.1670818.

[14] Nemirovsky N, van Rooji L. A New Methodology for Biofidelic Head-Neck-Postural Control. In: Proceedings of the IRCOBI Conference, 2001, 18.

[15] Kennedy J, van Eberhart RC. Particle Swarm Optimization. In: Proceedings of the IEEE International Conference on Neural Networks. Perth, Australia, 2001, 1942–1945.

[16] Happee R, de Bruijn E, Forbes PA, van Drunen P, van Dieën JH, van der Helm FCT. Neck postural stabilization, motion comfort, and impact simulation. In: Scataglini S, Paul G, editors. DHM and Posturography. Academic Press, 2019, 243–260.

[17] Kleinbach C, Martynenko O, Promies J, Haeufle DFB, Fehr J, Schmitt S. Implementation and Validation of the Extended Hill-Type Muscle Model with Robust Routing Capabilities in LS-DYNA for Active Human Body Models. BioMedical Engineering OnLine, 2017, 16(109), 1–28.